IEICE TRANS. COMMUN., VOL.E96–B, NO.10 OCTOBER 2013

INVITED PAPER *Special Section on Recent Progress in Antennas and Propagation in Conjunction with Main Topics of ISAP2012*

Electromagnetic Modeling of Metamaterials*

Toru UNO[†a)], ***Member***

SUMMARY Metamaterials are generally defined as a class of artificial effective media which macroscopically exhibit extraordinary electromagnetic properties that may not be found in nature, and are composed of periodically structured dielectric, or magnetic, or metallic materials. This paper reviews recently developed electromagnetic modeling methods of metamatericals and their inherent basic ideas, with a focus on full wave numerical techniques. Methods described in this paper are the Method of Moments (MoM) and the Finite Difference Time Domain (FDTD) Method for scattering problems excited by an incident plane wave and a single nonperiodic source, and the Finite Element Method (FEM), the Finite Difference Frequency Domain (FDFD) method and the FDTD method for band diagram calculations.

key words: *Metamaterials, Periodic Structure, Method of Moments, FDTD method, FEM, FDFD method, electromagnetic scattering, band diagram*

1. Introduction

Electromagnetic metamaterials, often called simply as metamaterials, have been generally defined as a class of artificial media or artificial materials which exhibit novel characteristics that may not be found in nature. Some researchers have a tendency to expand the concept of metamaterials so as to make it as broad as possible, and claim that semiconductor materials and/or devices should be classified as metamaterials, however this paper covers only a popularly accepted classification that metamaterials are made of the artificial material that Maxwell equations' macroscopic property is really dominant. That is, metamaterials are not ordinary materials made of natural molecules but are periodic structures composed of dielectric, or magnetic, or metallic materials. A periodicity of the structual elements is usually smaller than a half of wavelength, and each element is designed separately so as to realize a desired property as a whole.

The use of artificial periodic structures, i.e., metamaterials, has been investigated for antennas, microwave devices, and many other applications in the optical region. Examples include the creation of artificial dielectrics, artificial magnetism and superlens devices as well as electromagnetic band gap (EBG) structures that are used to suppress surface-wave propagation. In other applications, the metamatrial has been used to create an artificial magnetic conductor (AMC), and placing an antenna near the AMC has been used to realize low-profile antennas. It has also been demonstrated that the metamaterial can be used to create a high-directivity leaky-wave antenna. Other applications of metamaterials at microwave and optical frequencies can be seen in some books and papers listed in References. Author suggests the reader to look at these and references therein for complete understanding of recent progress of metamatericals [1]–[5].

The purpose of this paper is to review recently developed computational methods used for the electromagnetic field analysis in the presence of metamaterial structure. For simplicity and for the sake of brevity, we mainly deal with the most common case of a structure that is periodic in one or two directions. While the three-dimensional periodicity is rarely considered in the practical applications, it is analogous to 1D and 2D cases. To reduce computational resources, it is naturally desirable to apply periodic boundary conditions (PBCs) in electromagnetic modeling. PBCs are formulated in the spectral domain and have been implemented in several frequency domain techniques such as the Method of Moments (MoM) [6], [7], the Finite Element Method (FEM) [8] and so on. The Finite Difference Time Domain (FDTD) method [9]–[11] is also applied to such problems widely because of its straightforwardness to calculate the electromagnetic fields. Fortunately the spectral domain approaches have been successfully introduced into the FDTD method [1], [4], [11].

In Sect. 2, we will provide two different electromagnetic modeling methods of scattering fields for infinite periodic structures that are excited by a plane wave. After reviewing the MoM including the spectral PBC, we present some useful techniques to improve a computational efficiency for the method. This section also describes the FDTD techniques developed for the modeling of periodic structures including the pulsed plane wave at oblique incidence. Electromagnetic fields indicate no longer a periodic property when the metamaterial is excited by a single, i.e., a nonperiodic source. In order to overcome this difficulty, the array scanning method (ASM) was introduced. Using the ASM, the spectrum PBCs can successfully be integrated with the FDTD method in Sect. 3. On the other hand, basic characteristics of wave propagation in the metamaterials is generally described by their dispersion diagram connecting a wavenumber and an eigen-frequency. In Sect. 4, we provide how to calculate the dispersion diagram of the metamaterial using the FEM, or the Finite Difference Frequency Domain method [12] or the FDTD method.

Manuscript received May 8, 2013.

[†]The author is with the Graduate School of Engineering, Tokyo University of Agriculture and Technology, Koganei-shi, 184-8588 Japan.

*This work was supported in part by JSPS KAKENHI Grant Number 22109002.

a) E-mail: uno@cc.tuat.ac.jp

DOI: 10.1587/transcom.E96.B.2340

2. Plane Wave Scattering

We start with a brief summary of the standard Floquet or Bloch representation of the field in the periodic structure. This serves as a background for the succeeding sections. For simplicity, we consider two-dimensionally periodic structure that is periodic along x- and y-directions, and layered along the z-direction. Assuming that its periodicity is specified by a vector $\boldsymbol{L} = L_x\hat{\boldsymbol{x}} + L_y\hat{\boldsymbol{y}}$, and that the electromagnetic fields in it is either excited by an incident plane wave as discussed in this section, or due to a guided mode in Sect. 4, all of the electromagnetic quantities including an electric field $\boldsymbol{F}$ can be expressed by the Floquet or Bloch theory as

$$\boldsymbol{F}(\boldsymbol{r} + \boldsymbol{L}) = \boldsymbol{F}(\boldsymbol{r})e^{-j\boldsymbol{k}_t\cdot\boldsymbol{L}} \tag{1}$$

where $\boldsymbol{k}_t = k_x\hat{\boldsymbol{x}} + k_y\hat{\boldsymbol{y}}$ is a transverse wavenumber vector and $\boldsymbol{r}$ is an arbitrary position vector for fields, or the vector that specifies the position of the electric or magnetic current. A phase shift $\boldsymbol{k}_t \cdot \boldsymbol{L}$ appeared in Eq. (1) is expressed as, for exapmle, $\boldsymbol{k}_t \cdot \boldsymbol{L} = k_x L_x = k_0 L \sin\theta$ in one dimensional case as illustrated in Fig. 1.

2.1 Method of Moments

In this section, the basic scheme of MoM calculation for solving scattering problems of the periodic structures is briefly reviewed. To illustrate the concept, let us consider the example shown in Fig. 1, where the plane wave is incident on infinitely lined up scatterers V surrounded by S in free space. Since the scattering electric field $\boldsymbol{E}^{scat}(\boldsymbol{r})$ can be represented by a superposition of the field generated by an element current $\boldsymbol{J}(\boldsymbol{r}')$ on S or in V inside an unit cell bounded by a periodic boundary $\mathrm{P_B}$ and the current replicas in all the other unit cells, applying Eq. (1) to $\boldsymbol{J}(\boldsymbol{r})$, it is given as follows.

$$\boldsymbol{E}^{scat}(\boldsymbol{r}) = -jk_0 Z_0 \int_S \overline{\overline{G}}_p(\boldsymbol{r};\boldsymbol{r}')\cdot\boldsymbol{J}(\boldsymbol{r}')\,dS \tag{2}$$

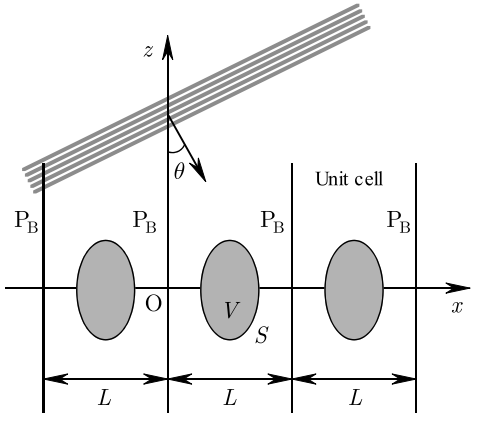

Fig. 1 Infinite periodic structure excited by incident plane wave. $\mathrm{P_B}$ indicates a periodic boundary, L is a period along the x-directon.

where $\overline{\overline{G}}_p(\boldsymbol{r};\boldsymbol{r}')$ is referred as a periodic Green's function and is expressed using a free space dyadic Green's function $\overline{\overline{G}}_0(\boldsymbol{r};\boldsymbol{r}')$ as

$$\overline{\overline{G}}_p(\boldsymbol{r};\boldsymbol{r}') = \sum_{m=-\infty}^{\infty} \overline{\overline{G}}_0(\boldsymbol{r};\boldsymbol{r}' + m\boldsymbol{L})e^{-jm\boldsymbol{k}_t\cdot\boldsymbol{L}} \tag{3}$$

The integral equation (IE) for the unknown current $\boldsymbol{J}$ on the surface of the perfect conductor, for example, can be derived from a boundary condition $\hat{\boldsymbol{n}} \times \left\{\boldsymbol{E}^{inc} + \boldsymbol{E}^{scat}\right\} = 0$, where $\hat{\boldsymbol{n}}$ is an unit normal vector on S. The use of the periodic Green's function (3) reduces the solution domain of the IE to only a single unit cell. However, the convergence of the space-domain series in Eq. (3) is very slow, and usually thousands or tens of thousands of terms must be summed up to attain acceptable accuracy. Alternatively, the convergency of the spectral-domain Green's function would rather good than the space-domain series, however the above drawback cannot completely be resolved. For this reason, intensive research has been carried out to accelerate the series in the periodic Green's function, and several techniques have been developed [7]. Particularly the Edward method [13] provides excellent computational efficiency [14].

2.2 FDTD Method

The FDTD method has been recognized as an extremely easy-to-use technique comparing with other computational methods, and is widely used to analyze many kinds of metamaterials. In this section, some FDTD modeling techniques for periodic structures are briefly reviewed on the assumption that the reader has already known well the fundamental scheme of the FDTD method.

Let us consider again the scattering problem as illustrated in Fig. 1 for simplicity. When Eq. (1) is transformed into the time domain, the electric or magnetic field $\boldsymbol{F}(\boldsymbol{r}, t)$ satisfies

$$\boldsymbol{F}(x, y, z, t) = \boldsymbol{F}(x + L, y, z, t + L\sin\theta/c) \tag{4}$$

where c is a light speed. This relation implies that the field data in the *future time* $t + L\sin\theta/c$ are needed to update the electromagnetic fields in the *current time* t. This is a fundamental difficulty in applying the original FDTD method to the periodic structures. To overcome this difficulty, various approaches have been proposed. Before introducing the basic concept of these method, we treat the fundamental case of normal plane wave incidence in this section.

A schematic view of a computational space within the single unit cell for the scattering analysis is illustrated in Fig. 2. The computational space is enclosed by absorbing boundaries (ABs) on the top and bottom and $\mathrm{P_B}$ on four sides. The perfectly matched layers (PMLs) [15] are usually used as ABs for achieving the excellent calculation accuracy. A plane wave source is putted uniformly on a surface $\mathrm{S_E}$ above the petiodic structure. An observation plane $\mathrm{S_O}$ is set at an appropriate position to extract the scattered field. It

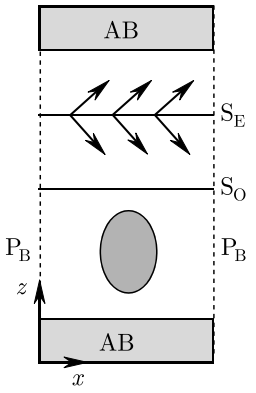

Fig. 2 Computational space in a single unit cell used to the FDTD scattering analysis for plane wave incidence.

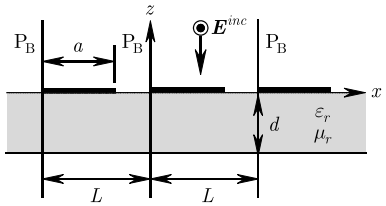

(a) Periodic metal strip on dielectric slab

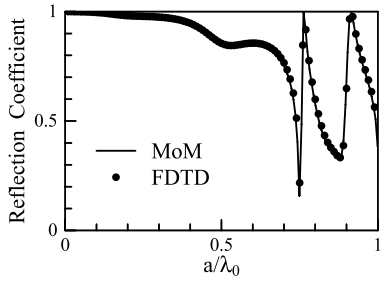

(b) Reflection coefficient

Fig. 3 Reflection coefficients computed by the FDTD method and the MoM. $\varepsilon_r = 2, \mu_r = 1, L = 2a, d = \lambda_0$.

is noted here that Fig. 2 iillustrates the computational space for the total-field representation. The scattered-field representation or their combined method [9]–[11] is also available for this analysis.

2.2.1 Normal Incidence

When the plane wave is normally incident on the periodic structure, we have $\theta = 0$. Therefore, it is clear from Eq. (4) that no data in the future time is needed. Hence, the PBC (4) can easily be combined with the original FDTD method. The periodic boundary P_B is treated as a perfect electric or magnetic wall depending on the polarization of incident electric field.

An example is shown in Fig. 3. Figure 3(a) shows an infinitely periodic conducting strip backed by an uniform dielectric slab. The strips are assumed to be infinitely long in the y-direction. A $y-$ polarized plane wave propagating along the z-direction illuminates normally on the slab-strip structure. The computed reflection coefficient is shown in Fig. 3(b), where λ_0 is a free space wavenumber. The FDTD results agree excellently well with the results obtained from the Galerkin's MoM described in the preceding subsection. In the MoM simulation [16], the Green's function for the dielectric slab was used instead of the free space Green's function in Eq. (3). A roof-hat function was chosen as a test function. In this problem, the spectral representation of the Green's function was very useful to reduce the computational cost.

2.2.2 Oblique Incidence: Early Works

The difficulty of the time shift condition (4) can be removed when the electromagnetic fields are excited by a sinusoidal time dependence wave, that is $e^{j\omega t} = \cos\omega t + j\sin\omega t$. This is a basic idea of a Sine-Cosine method [17]. In this method, the computational space is excited by two plane waves: one with $\cos\omega t$ and the other with $\sin\omega t$. Let us denote the corresponding electric and magnetic fields as $\boldsymbol{F}_r$ and $\boldsymbol{F}_m$ simply. The conventional Yee's algorithm is applied to update these two sets of fields separately. If we combine these field as $\boldsymbol{F} = \boldsymbol{F}_r + j\boldsymbol{F}_m$, then the combined complex field is equivalent to the field excited by $e^{j\omega t}$. Therefore, the Floquet condition (1) can be applied directly to this combined field $\boldsymbol{F}$ at the PBs facing each other. Finally two set of fields for $\cos\omega t$ and $\sin\omega t$ are obtained from $\boldsymbol{F}$ as $\boldsymbol{F}_r = \Re(\boldsymbol{F})$ and $\boldsymbol{F}_m = \Im(\boldsymbol{F})$. This procedure is repeated in each time step until the steady state is reached.

This method can be applied to wide variety of scattering problems without modifying the original Yee's algorithm, however it loses the wideband capability of the FDTD method because all of the calculation procedures are performed at a single frequency. To improve the computation efficiency, a split-field technique [18] was proposed basing on the field transformation technique [19]. This technique allows us to use the pulsed plane wave, however the stability condition for a cubic cell with the size of Δx is modified as

$$\frac{c\Delta t}{\Delta x} \leq \frac{1 - \sin\theta}{\sqrt{D}} \tag{5}$$

where D is the dimensionality of the problem. It is found from Eq. (5) that the required time step Δt must become smaller as the incident angle θ increases. Therefore, Δt becomes so tiny that the FDTD simulation time is prohibitively long when the incident angle approaches to the grazing angle.

2.2.3 Oblique Incidence: Unified Spectral FDTD Method

The Sine-Cosine method has been developed so as to simultaneously analyze both the plane wave scattering problem and the guided wave problem in a simple and unified manner [20]. Furthermore, the auto-regressive moving-average

(ARMA) estimator [21], [22] conventionally used in the signal processing area has recently been implemented so that it is capable to calculate the time domain responses efficiently.

Let us consider first the case of the single frequency excitation that the time dependence is expressed by $e^{j\omega t}$. Denoting again the wavenumbers along the x- and y-directions as k_x and k_y,respectively, then, for given free space wavenumber $k_0 = \omega/c$, $k_t^2 = k_x^2 + k_y^2 \le k_0^2$ means that the plane wave propagates along a direction specified by $\boldsymbol{k} = \boldsymbol{k}_t + k_z\hat{\boldsymbol{z}}$ where $k_z = \sqrt{k_0^2 - k_t^2}$. Contrarily, $k_t > k_0$ provides the guided wave that propagates along the horizontal direction and decays exponentially in the z-direction. In this case the eigenmodes and eigenfrequencies of the structures are of general interest. Therefore, if we keep $\boldsymbol{k}_t$ at the spacified value and vary k_0, the field phenomena in the regions from the guided wave to the plane wave can be treated. Thus, the unified spectral FDTD method described here, often called a constant-k FDTD method, calculates the electromagnetic behavior at given horizontal wave numbers but different incident angles. It is noted here that the incident angle θ of the plane wave in the scattering problem is obtained from the relation $k_0 \sin\theta = k_t$. Therefore, varying the frequency or k_0 for a fixed $\boldsymbol{k}_t$ results in different incident angles.

As mentioned above, Eq. (1) is satisfied in the time domain as well for this case and can be rewritten by adding the time t as

$$\boldsymbol{F}(\boldsymbol{r} + \boldsymbol{L}, t) = \boldsymbol{F}(\boldsymbol{r}, t)e^{-j\boldsymbol{k}_t \cdot \boldsymbol{L}} \tag{6}$$

Note that $e^{-j\boldsymbol{k}_t \cdot \boldsymbol{L}}$ is a constant number in Eq. (6), resulting in complex values for both electric and magnetic fields. Since no time delay or advancement is required in this equation, the conventional Yee's scheme can be used to update the electromagnetic fields in the computational space. In addition, since Eq. (6) is true for a given frequency and given $\boldsymbol{k}_t$, it still holds when a wideband pulse is launched into the space, by the superposition of all frequency components.

It may be instructive to overview the previous four periodic conditions on the $k-\omega$ plane as illustrated in Fig. 4 in which the abscissa indicates k_x or k_y, or k_t. The normal incident case that $\theta = 0$ and $k_t = 0$ corresponds to the leftmost line. The sine-cosine method which calculates the fields at oblique incidence but only a single frequency, is indicated by a black point. The wideband split-field method calculation is performed at a given incident angle, as represented by the tilted line. On the other hand, the unified spectral method or the constant-k method corresponds to the vertical line with the constant wavenumber.

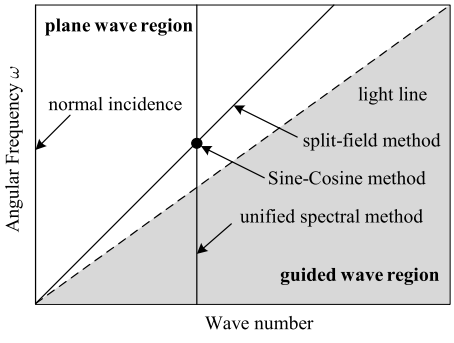

Fig. 4 $k-\omega$ plane.

The unified spectral method has significantly enhanced both the capability and the availability of the FDTD method on the theoretical point of view, however numerical instability in the time domain computation often occurs on some specific problems. For example, if the periodic strip on the dielectric stab as shown in Fig. 3 is excited by the obliquely incident plane wave at the eigenfrequencies, the surface wave are guided along the horizontal directions. The energy exiting the computational space at the one periodic boundary P_B reenters the space at other boundary following the periodic boundary condition. Consequently, the time domain data does not decay to zero. As a consequence, accurate frequency domain properties cannot be obtained through the usual Fourier transformation. To solve this problem efficiently, the ARMA estimator has been implemented into the unified spectral FDTD method. Assuming the problem to be analyzed is a linear system with the transfer function;

$$H(z) = \frac{a_0 + a_1 z^{-1} + a_2 z^{-2} + \cdots + a_q z^{-q}}{1 + b_1 z^{-1} + b_2 z^{-2} + \cdots + b_p z^{-p}} \tag{7}$$

where $z = e^{j\omega t}$, the time domain data at $t = n\Delta t$ can be expressed by the early time domain data as

$$y(n) = -\sum_{i=1}^{p} b_i y(n-i) + \sum_{j=0}^{q} a_j x(n-j) \tag{8}$$

where $x(n)$ and $y(n)$ are input and output signals, and corresponds to, for example, the incident and scattered electric fields, respectively. a_j and b_i are unknown coefficients to be determined from these data.

To check the computational accuracy, the frequency characteristics of reflection coefficient for the dielectric slab are analyzed by the unified spectral FDTD/ARMA hybrid method (US-FDTD/ARMA), by dividing the original geometry into a series of periodic cells. The thickness d and the relative permittivity ε_r are set 7.5 mm, 4, respectively. The

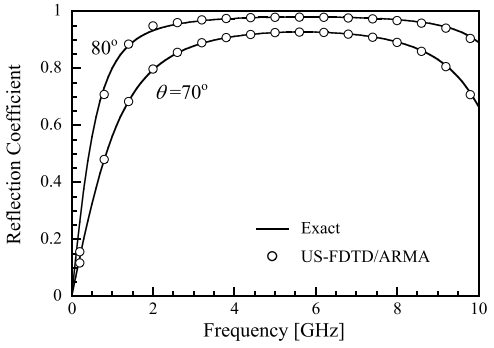

Fig. 5 Reflection coefficient of dielectric slab for obliquely incident plane wave.

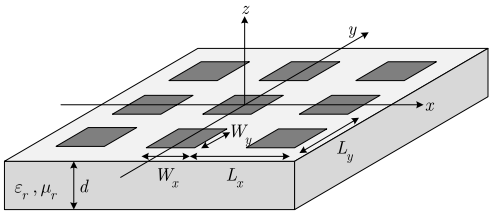

(a) Infinite periodic rectangular metal plate on dielectric slab

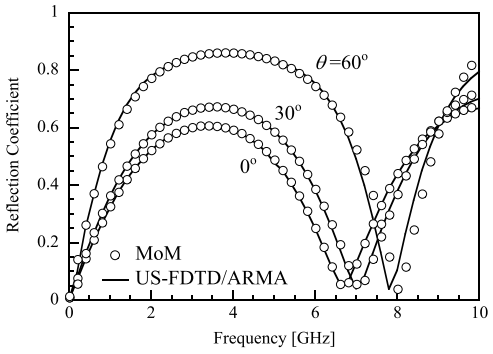

(b) Reflection coefficient

Fig. 6 Comparison of reflection coefficient computations using MoM and US-FDTD/ARMA hybrid technique.

incident plane wave was TE wave. The results for two incident angles are shown in Fig. 5. It is found that this method has good accuracy even if the incident angle is very close to the grazing angle.

Alternative example is an infinite periodic rectangular conducting plate located on the dielectric slab as illustrated in Fig. 6(a). The plane wave that has y-polarized electric field, is obliquely incident on the structure from the positive $z-$ axis with the angle θ. The calculated frequency characteristics of the reflection coefficient are shown in Fig. 6(b). We set $L_x = L_y = 8\,\text{mm}$, $W_x = W_y = 4\,\text{mm}$, $d = 10\,\text{mm}$, $\varepsilon_r = 4$, $\mu_r = 1$. It is noted here that the tangential scattered electric field is corrected on the observation plane S_O indicated in Fig. 2, and its amplitude is extracted by averaging these data as following with the phase delay being considered;

$$E_s = \frac{1}{S_O}\int_{S_O} E(x,y)e^{j(k_x x+k_y y)}\,dS \tag{9}$$

It is found that the US-FDTD/ARMA hybrid method agrees well with the MoM, demonstrating the good accuracy of the method.

3. Single Source on Periodic Structure

All of the methods described above assume that the periodic structures are illuminated by planar electromagnetic fields. That is, these methods are valid only when the incident signal is also periodic. For some applications in which electromagnetic responses from an arbitrary antenna are required, the so called "brute-force" simulations have often been performed. In this simulation, a number of unit cells are usually required to reduce a significant reflection from boundaries truncating the actual infinite periodic structure. This approach often requires significant computational resources depending on the antenna shape, the physical quantities of interest and so on.

In this section, we briefly review how the field excited by the single, that is, the nonperiodic dipole source in the presence of the infinite periodic structure is calculated by the array scanning method (ASM). The ASM has originally been introduced in the analysis of phased array antenna [23], [24] and used in various types of metamaterials in recent years [1]. A direct plane-wave expansion method (PWEM) is available for analyzing this geometry, and some techniques described in the preceding sections may be applicable, however, it is known that the ASM is more efficient than the PWEM.

The basic idea of the ASM originates in the fact that the dipole moment density of the single dipole source $\boldsymbol{p}(\boldsymbol{r})$ at $\boldsymbol{r}_0$ that is oriented along the vector $\boldsymbol{p}_0$, can be synthesized by a superposition of infinite phased arrays of identical point sources located at $\boldsymbol{r}_{mn} = \boldsymbol{r}_0 + mL_x\hat{\boldsymbol{x}} + nL_y\hat{\boldsymbol{y}}$. Mathematically, $\boldsymbol{p}(\boldsymbol{r})$ can be obtained by integrating over the Brillouin zone as

$$\begin{aligned}\boldsymbol{p}(\boldsymbol{r}) &= \boldsymbol{p}_0\delta(\boldsymbol{r}-\boldsymbol{r}_0)\\ &= \frac{L_xL_y}{(2\pi)^2}\int_{-\frac{\pi}{L_x}}^{\frac{\pi}{L_x}}\int_{-\frac{\pi}{L_y}}^{\frac{\pi}{L_y}}\boldsymbol{p}^{\infty}(\boldsymbol{r},\boldsymbol{k}_t)\,dk_x\,dk_y\end{aligned} \tag{10}$$

The phased array of dipole sources $\boldsymbol{p}^{\infty}$ is represented as

$$\boldsymbol{p}^{\infty}(\boldsymbol{r},\boldsymbol{k}_t) = \boldsymbol{p}_0\sum_{m=-\infty}^{\infty}\sum_{n=-\infty}^{\infty}\delta(\boldsymbol{r}-\boldsymbol{r}_{mn})e^{-j\boldsymbol{k}_t\cdot\boldsymbol{d}_{mn}} \tag{11}$$

where $\boldsymbol{d}_{mn} = mL_x\hat{\boldsymbol{x}}+nL_y\hat{\boldsymbol{y}}$. Since the superposition principle holds for the sources, it holds for the generated fields. Thus the electric field $\boldsymbol{E}(\boldsymbol{r})$ excited by the single source can be synthesized by superimposing the electric fields produced by all of the phased array sources $\boldsymbol{p}_0e^{-j(mk_xL_x+nk_yL_y)}$ at $\boldsymbol{r}_{mn}$. If we denote the superposed field as $\boldsymbol{E}^{\infty}(\boldsymbol{r},\boldsymbol{k}_t)$, $\boldsymbol{E}(\boldsymbol{r})$ is mathematically expressed as

$$\begin{aligned}\boldsymbol{E}(\boldsymbol{r}+\boldsymbol{d}_{mn}) = \frac{L_xL_y}{(2\pi)^2}&\int_{-\frac{\pi}{L_x}}^{\frac{\pi}{L_x}}\int_{-\frac{\pi}{L_y}}^{\frac{\pi}{L_y}}\\ &\boldsymbol{E}^{\infty}(\boldsymbol{r},\boldsymbol{k}_t)e^{-j\boldsymbol{k}_t\cdot\boldsymbol{d}_{mn}}\,dk_x\,dk_y\end{aligned} \tag{12}$$

where $\boldsymbol{r}+\boldsymbol{d}_{mn}$ indicate the observation point in the (m,n)-th unit cell and $\boldsymbol{r}$ lies within the reference unit cell, that is the $(0,0)$-th cell. Obviously $\boldsymbol{E}^{\infty}(\boldsymbol{r},\boldsymbol{k}_t)$ satisfy the periodic boundary condition (6).

Using the ASM and the MoM scheme described in Sect. 2.1, some interesting properties of dipole scattering by periodic materials has been investigated [25], [26], however, for the arbitrary shaped antenna, a sophisticated MoM approach has not been developed yet due to its own complexity, finite computer resources and so on.

It may be easily understood for the reader that the ASM can be implemented into the FDTD method. Performing

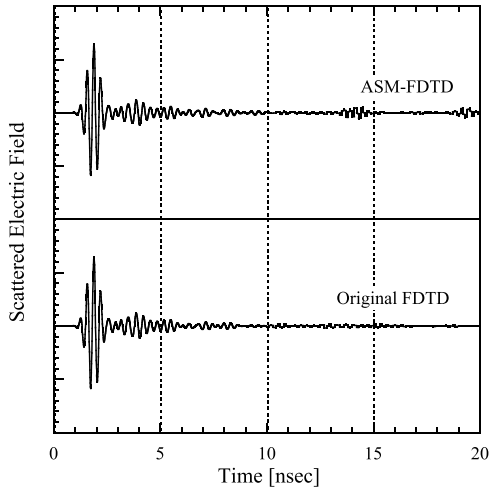

Fig. 7 Scattered electric fields calculated by ASM-FDTD and original FDTD.

the unified spectral FDTD simulations using the periodic boundary condition (6) for different wave numbers of k_x and k_y, we can find the field $\boldsymbol{E}^{\infty}(\boldsymbol{r}, \boldsymbol{k}_t, t)$ excited by the infinite periodic source array. The time domain field is obtained by integrating $\boldsymbol{E}^{\infty}(\boldsymbol{r}, \boldsymbol{k}_t, t)$ over the Brillouin zone. An example is shown in Fig. 7. This shows the scattered electric fields calculated by the ASM-FDTD method and the original, that is, brute-force FDTD method. The geometry of the problem is the same as Fig. 6(a) in which all sizes are enlarged 10 times as the example of Fig. 6(b). The dipole source oriented along the z-axis is placed at $z = 100$ mm, and is excited by the sinusoidally modulated Gaussian pulse. The observation point separates T_x along y axis from the source point. 11×11 unit cells are included in the computational space in the original FDTD simulation. This is large enough to reduce the truncation error to an extremely small value. The integration over k-space in the ASM-FDTD was performed by simply summing up 48×48 sampling data in the $k_x - k_y$ domain. It is observed in Fig. 7 that the early time responses are very similar each other, but small noises appears around 14 nsec and 19 nsec in the ASM-FDTD. This distortion is caused from the image sources regarding the k-space integration. Therefore, the spectral sampling rate must be carefully selected in the ASM-FDTD simulations.

4. Dispersion Diagram

Wavenumber k is an important parameter to describe the propagation property of electromagnetic waves such as the phase and group velocities, and the field distribution as well. It is usually difficult to give an explicit expression for the wavenumber, therefore one has to perform a full wave simulation to determine it numerically. The relation between k or phase constant and ω is often referred to as the dispersion diagram. In this section, we describe how the dispersion diagram of the periodic structure is computed. We deal with the 2-D case for simplicity, but the development to 3-D is easy and straightforward.

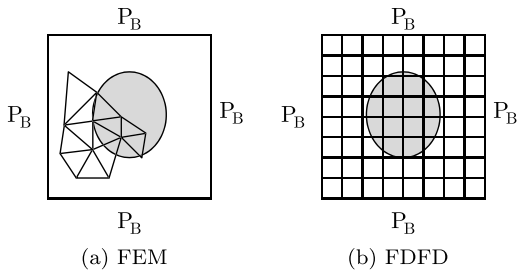

Fig. 8 Lattice structures in unit cell.

4.1 FEM and FDFD Method

Computational schemes of both the FEM and the FDFD are very similar and straightforward. Electromagnetic fields are calculated using the weighted residual method for the differential wave equation based on the polynominal approximation in the FEM. On the other hand, the FDFD method is based on the finite difference approximation of Maxwell's curl equations. Applying the periodic boundary condition (1) to four periodic boundaries $\mathrm{P_B}$ shown in Fig. 8, we can obtain the equation

$$A\boldsymbol{x} = \omega B\boldsymbol{x} \tag{13}$$

for both methods, where the elements of the matrices A and B are determined by the constitutive parameters, the structural parameters of the lattice and $\boldsymbol{k}_t$, and the vector $\boldsymbol{x}$ represents the values of the field at the lattice points. Thus, the dispersion diagram can be obtained by solving the eigenvalue problem (13). Therefore this approach seems to be simple, however the computational accuracy depends on the lattice size. Furthermore, the size of the matrix equation (13) increases impractically for 3-D case because the dimension of $\boldsymbol{x}$ is identical with the number of lattice points. Although the FDFD method has these disadvantages, it is attractive as the computational technique, and is recently developed to the frequency dispersive material [27].

4.2 FDTD Method

The dispersion diagram can be calculated by the unified spectral FDTD method as well. The space in the unit cell surrounded by the periodic boundaries $\mathrm{P_B}$s is excited by the electric or magnetic line source located at an arbitrary point in it for the pair of the fixed wave wavenumber (k_x, k_y). The field is observed at a different point in the same unit cell. An example of the observed electric field data is shown in Fig. 9(a), for the source excited by the Gaussian pulse modulated by the sinusoidal wave. Performing the Fourier transformation numerically, that is, using the FFT, we can obtained the frequency spectrum as shown in Fig. 9(b) The dispersion diagram can be plotted by repeating the above calculations for the different wavenumber pair. Figure 10 illustlates the dispersion diagram composed of the dielectric cylinder with $\varepsilon_r = 8.9$. For comparison, the results obtained

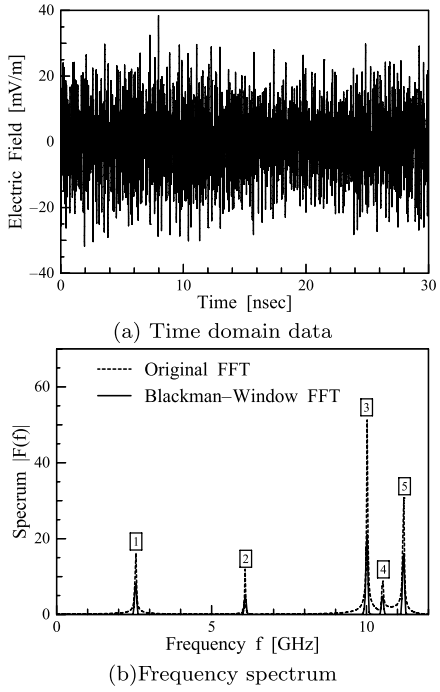

Fig. 9 Observed electric field.

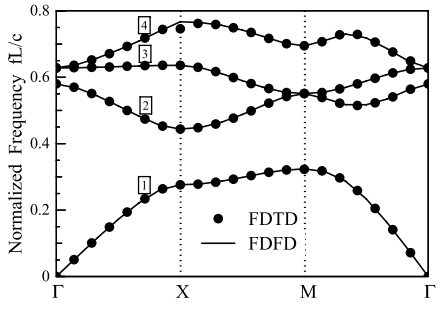

Fig. 10 Dispersion diagram of photonic clystal composed of dielectric cylinder.

from the FDFD method described above, is also shown [28]. In this figure, three points Γ, X, and M on the abscissas denote $(k_x, k_y) = (0, 0), (\pi/L_x, 0), (\pi/L_x, \pi/L_y)$ in the Brillouin zone, respectively.

The plane wave can be used for the excitation of the space instead of the point source. In this case, the similar spectrum as Fig. 9(b) can also be obtaied by calculating the correlation between the observed field and the incident plane wave.

It is noted here that the Filter Diagonalization Method (FDM) is more efficient than the FFT for detecting the peaks of the spectrum, for both the computational accuracy and the requited computational time [29], [30]. It is also noted that we cannot distinguish whether the mode is the degenerated one or not, only from the spectrum as shown in Fig. 9(b). For solving this difficulty, novel approach based on the group theory has been proposed recently [31].

5. Conclusion

This paper has reviewed recently developed electromagnetic modeling methods of metamatericals with a focus on full wave numerical techniques that are based on the MoM and the FDTD method for scattering problems excited by the plane wave and the single nonperiodic source. The FEM, the FDFD method and the FDTD method for the dispersion diagram calculations were also viewed. We have devoted a good deal of space to the FDTD method because it is recently used to the analysis and design of metamaterials very frequently as compared to other methods

We could not mention other important numerical methods and applications of metamaterials as space is limited. Author suggests the reader to consult some books and/or papers listed in the Reference and references therein.

References

[1] P. Capolono, ed., Metamaterials Handbook, Part I: Theory and Phenomena of Metamaterials, Part II: Applications of Metamaterials, CRC Press, 2009.
[2] T. Ishihara, A. Sanada, and K. Kajiwara, ed., Metamaterial II, CMC Publ. Co., Ltd. 2012 (In Japanese).
[3] C. Caloz and T. Itoh, Electromagnetic Metamaterials: Transmission Line Theory and Microwave Applications, John Wiley & Sons, 2006.
[4] F. Yang and Y. Rahmat-Samii, Electromagnetic Band Gap Structures in Antenna Engineering, Cambridge Univ. Press, 2009.
[5] N. Engheta and R.W. Ziolkowski, Metamaterials: Physics and Engineering Explorations, John Wiley & Sons, 2006.
[6] W.C. Gibson, The Method of Moments in Electromagnetics, Chapman & Hall/CRC, 2008.
[7] A.F. Peterson, et al., Computational Methods for Electromagnetics, IEEE Press, 1998.
[8] J.L. Volakis, et al., Finite Element Method for Electromagnetics, IEEE Press, 1998.
[9] T. Uno, Finite Difference Time Domain Method for Electromagnetics and Antennas, Corona Publ. Co., Ltd, 1988 (in Japanese).
[10] A. Taflove, Computational Electrodynamics: The Finite-Difference Time-Domain Method, 3rd ed., Artech House, 2005.
[11] Y. Hao and R. Mittra, FDTD Modeling of Metamaterials, Theory and Application, Artech House, 2009.
[12] K. Yasumoto, Electromagnetic Theory and Applications for Photonic Crystals, CRC Press, 2006.
[13] P.P. Edward, "The calculation of optical and elecytrostatic potential," Ann Phys., vol.64, no.3, pp.253–287, 1921.
[14] G. Lovat, P. Burghignoli, and R. Ananero, "Efficient evaluation of the 3-D periodic Green's function through the edward method," IEEE Trans. Microw. Theory Tech., vol.56, no.9, pp.2069–2075, Sept. 2008.
[15] J.-P. Berenger, "A perfectly matched layer for the absorption of electromagnetic waves," J. Comput. Phys., vol.114, no.1, pp.185–200, 1994.
[16] M. Ide, T. Uno, Y. Kushiyama, and T. Arima, "Fast method of moments calculation of electromagnetic plane wave scattering due to periodic conducting strips backed by a dielectric slab," IEICE Trans. Commun. (Japanese Edition), vol.J94-B, no.9, pp.1086–1093, Sept. 2011.
[17] P. Harms, R. Mittra, and W. Ko, "Implementation of the periodic boundary condition in the finite-difference time-domain algorithm for FSS structures," IEEE Trans. Antennas Propag., vol.42, pp.1317–1324, 1994.

[18] J.A. Roden, et al., "Time-domain analysis of periodic structures at oblique incidence: Orthogonal and nonorthogonal FDTD implementations," IEEE Trans. Microw. Theory Tech., vol.46, no.4, pp.420–427, April 1998.
[19] M.E. Veysogle, R.T. Shin, and J.A. Kong, "A finite-difference time-domain analysis of wave scattering from periodic surfaces," J. Electromagn. Waves Appl., vol.7, pp.1595–1607, 1993.
[20] A. Aminian, F. Yang, and Y. Rarmat-Samii, "Bandwidth determination for soft and hard ground planes by spectral FDTD: A unified approach in visible and surface wave regions," IEEE Trans. Antenans Propag., vol.53, no.1, pp.18–28, Jan. 2005.
[21] L.B. Jackson, Digital Filters and Signal Processing, Kluwer, Boston, MA, 1986.
[22] A.K. Shaw and K. Naishadham, "ARMA-based time-signiture estimator for analyzing resonant structures by the FDTD method," IEEE Trans. Antennas Propag., vol.49, no.3, pp.327–339, March 2001.
[23] R. Sigelmann and A. Ishimaru, "Radiation from periodic structures excited by an aperiodic source," IEEE Trans. Antennas Propag., vol.13, no.3, pp.354–364, May 1965.
[24] B.A. Munk and G.A. Burrell, "Plane-wave expansion for arrays of arbitrarily oriented piecewise linear elements and its application in determining the impedance of a single linear antenna in a lossy half-space," IEEE Trans. Antennas Propag., vol.27, no.3, pp.331–343, May 1979.
[25] E. Capolino, D.R. Jackson, and D.R. Wilton, "Fundamental properties of the field at the Interface between air and a periodic artificial material excited by a line source," IEEE Trans. Antennas Propag., vol.53, no.1, pp.91–99, Jan. 2005.
[26] E. Capolino, et al., "Comparison of methods for calculating the field excited by a dipole near a 2-D periodic material," IEEE Trans. Antennas Propag., vol.55, no.6, pp.1644–1655, June 2007.
[27] A.G. Hanif, T. Uno, and T. Arima, "Finite-difference frequency-domain algorithm for band diagram calculation of 2-D photonic crystals composed of debye type dispersive materials," IEEE Antennas Wireless Propag. Lett., vol.11, pp.41–44, 2012.
[28] A.G. Hanif, Y. Kushiyama, T. Uno, and T. Arima, "FDFD and FDTD methods for band diagram analysis of 2- dimensional periodic structure," IEICE Trans. Commun., vol.E93-B, no.10, pp.2670–2672, Oct. 2010.
[29] V.A. Mandelshtam and H.S. Tayer, "Harmonic inversion of time signal," J. Chem. Phys., vol.107, no.17, pp.6756–6769, 1997, A list of errata:vol.107, no.10, p.4128, 1998.
[30] G.A. Stark, et al., "Positional dependence of FDTD mode detection in photonic crystal systems," Int. J. Numer. Model., vol.209, pp.201–218, 2009. Program code is available at http://ab-initio.mit.edu/wiki/index.php/Harminv
[31] H. Sakamoto, T. Uno, T. Arima, and Y. Kushiyama, "Classification of degenerate and non-degenerate modes of photonic crystals in FDTD analysys by group theory," IEICE Communication Express, vol.2, no.5, pp.211–216, May 2013.

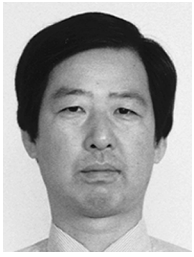

Toru Uno received the B.S. degree in Electrical Engineering from Tokyo University of Agriculture and Technology (TUAT), Tokyo, Japan, in 1980, and the M.S. and Ph.D. degrees in Electrical Engineering from Tohoku University, Sendai, Japan, in 1982 and 1985, respectively. In 1985 he was appointed as a Research Associate in the Department of Electrical Engineering of Tohoku University. From 1991 through 1994 he was an Associate Professor of the same university. He is presently a Professor in the Department of Electrical and Electronics Engineering of the TUAT. Since August 1998 through May 1999, he was on leave from the TUAT to join the Electrical Engineering Department at the Pennsylvania State University, University Park, PA, as a Visiting Scholar. He served as an associate-editor of the IEICE Transactions on Communications from 2000 to 2005, chair of Technical Group on Antennas and Propagation from 2011 to 2013, respectively. He also served as chair of IEEE AP-S Japan Chapter from 2003 to 2004. He is now an Associate Editor of IEEE Antennas and Wireless Propagation Letters. He received the Young Scientist Award, the Distinguished Contributions Award and the Paper Award, all from IEICE, in 1990, 2006 and 2007, respectively. His research interests include electromagnetic inverse problem, computational electromagnetics, medical and subsurface radar imagings, and electromagnetic compatibility. Dr. Uno is a senior member of IEEE, member of AGU and Japan Society for Simulation Technology.